# Modulation Format Identification in Coherent Receivers Using Deep Machine Learning

Faisal Nadeem Khan, Kangping Zhong, Waled Hussein Al-Arashi, Changyuan Yu, Chao Lu, and Alan Pak Tao Lau

***Abstract*— We propose a novel technique for modulation format identification (MFI) in digital coherent receivers by applying deep neural network (DNN) based pattern recognition on signals' amplitude histograms obtained after constant modulus algorithm (CMA) equalization. Experimental results for three commonly-used modulation formats demonstrate MFI with an accuracy of 100% over a wide optical signal-to-noise ratio (OSNR) range. The effects of fiber nonlinearity on the performance of MFI technique are also investigated. The proposed technique is non-data-aided (NDA) and avoids any additional hardware on top of standard digital coherent receiver. Therefore, it is ideal for simple and cost-effective MFI in future heterogeneous optical networks.**

***Index Terms*— Modulation format identification, coherent detection, deep machine learning.**

## I. Introduction

THE next-generation fiber-optic communication networks are envisioned to be flexible in nature whereby the available network resources can be allocated adaptively with the objective of maximizing the spectral and energy efficiencies [1]. Such elastic optical networks (EONs) are expected to be fully capable of dynamically adjusting various transmission parameters such as modulation formats, line rates, spectrum assignments etc., depending upon the changing traffic demands and network condition. One key requirement for digital coherent receivers in EONs is the capability to autonomously identify the modulation formats of received signals without any prior information from the transmitters. This vital information about signals' modulation formats can be fed forward to subsequent blocks in the digital signal processing (DSP) chain for improving their performances [2].

Over the last few years, a number of MFI techniques for digital coherent receivers have been proposed. These include: (i) method based on $k$-means algorithm [3], which performs MFI at the final stage of a DSP chain, thus demanding all the earlier algorithms to be modulation format-transparent; (ii) signal cumulants [4] and signal power distribution [5] based techniques, which assume prior information about OSNR of the received signal; (iii) method based on evaluation of peak-to-average-power ratio (PAPR) of received data samples [6], which necessitates additional hardware components such as filters, power meters etc., thus increasing the implementation complexity (and cost) significantly, particularly in scenarios where MFI needs to be performed at multiple locations in an optical network; and (iv) Stokes space representation and variational Bayesian expectation maximization (VBEM) algorithm-based technique [7], which employs an iterative framework for the optimization of certain set of parameters, thus requiring considerable computation time. This property may potentially be disadvantageous in EONs involving rapid switching of modulation formats.

Deep machine learning, also known as deep structured learning or hierarchical learning, is a new branch of machine learning which is based on the concept of distributed representation of data [8]. Deep learning architectures such as DNNs, deep convolutional neural networks (DCNNs), deep Boltzmann machines (DBMs) etc., exploit the fact that higher level features of data can be derived from lower level ones, resulting in a hierarchical representation of data. This property is somewhat similar to the one exhibited by human brain that appears to process information via several different levels of transformation and representation [9]. This behavior is particularly evident from human visual system which involves numerous hierarchical processing stages such as edges detection, primitive shapes formation, and proceeding gradually to construct more sophisticated visual shapes. Inspired by these characteristics, a deep learning architecture is comprised of several nonlinear processing layers (whose number defines the depth of architecture) performing automatic features extraction and transformation. The ability to extract and learn features at multiple levels of abstraction enables a deep learning system to learn complex relationships between inputs and outputs directly from the data instead of using human-crafted features.

Recently, we demonstrated the use of classical machine learning techniques namely artificial neural networks (ANNs) [10] and principal component analysis (PCA) [11], [12] for MFI in heterogeneous fiber-optic networks. However, since these methods exploit statistical properties of directly detected

Manuscript received March 25, 2016; revised May 2, 2016; accepted May 24, 2016. Date of publication June 1, 2016; date of current version June 30, 2016. This work was supported in part by the National Natural Science Foundation China under Grant 61401020 and Grant 61435006 and in part by the Hong Kong Government General Research Fund under Project PolyU152079/14E.

F. N. Khan, K. Zhong, C. Yu, C. Lu, and A. P. T. Lau are with the Photonics Research Centre, The Hong Kong Polytechnic University, Hong Kong (e-mail: fnadeem.khan@yahoo.com; zhongkangping1987@gmail.com; changyuan.yu@polyu.edu.hk; chao.lu@polyu.edu.hk; alan.pt.lau@polyu.edu.hk).

W. H. Al-Arashi is with the Department of Electronic Engineering, University of Science and Technology, Sana'a 13064, Yemen (e-mail: wal112005@yahoo.com).

Color versions of one or more of the figures in this letter are available online at http://ieeexplore.ieee.org.

Digital Object Identifier 10.1109/LPT.2016.2574800

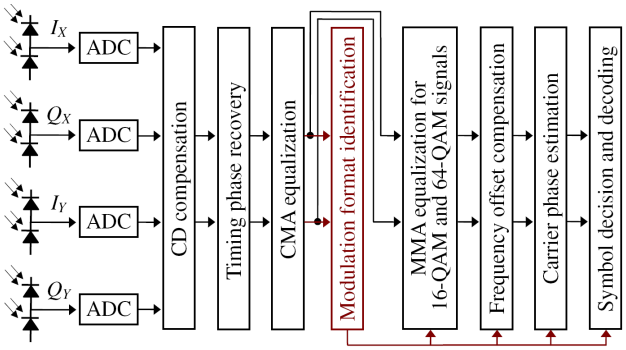


Fig. 1. Receiver DSP architecture with the proposed MFI stage shown in red color.

signals, they are not applicable to dispersion-uncompensated coherent optical systems. In this letter, we propose a novel technique which employs a DNN architecture to hierarchically extract a few representative features of signals' amplitude histograms obtained after CMA equalization in digital coherent receivers. These modulation format-sensitive features are then exploited by DNN for the identification of unknown signal types. The experimental results for 112 Gbps polarization-multiplexed (PM) quadrature phase-shift keying (QPSK), 112 Gbps PM 16 quadrature amplitude modulation (16-QAM), and 240 Gbps PM 64-QAM signals show that the proposed technique can enable accurate MFI in digital coherent receivers without necessitating any additional hardware as well as without requiring prior information about OSNR. Furthermore, since this technique is NDA, it does not have any adverse effect on spectral efficiency of the system. The proposed technique is non-iterative in nature and thus can facilitate fast MFI in future EONs.

## II. Operating Principle

The receiver DSP architecture, including the proposed MFI stage, is shown in Fig. 1. We employ conventional modulation format-transparent chromatic dispersion (CD) compensation and timing recovery algorithms followed by the CMA equalization which aims to compensate almost all linear transmission impairments. As clear from the figure, the proposed MFI technique processes signals at the output of CMA equalization stage. The information about signals' modulation formats, obtained through MFI, is passed to the subsequent DSP blocks such as multi-modulus algorithm (MMA) equalization for enabling modulation format-optimized processing. Figure 2 shows constellation diagrams and corresponding amplitude histograms for QPSK, 16-QAM, and 64-QAM signals after CMA equalization. It is obvious from the figure that the shapes of amplitude histograms are unique and contain distinctive signatures of these modulation formats. Although, the shapes of histograms do vary with OSNR, as clear from Fig. 2(b), they still remain distinguishable from each other. The modulation format-dependent features of amplitude histograms can be exploited for MFI by applying deep machine learning-based pattern recognition techniques.

In this work, we employed a two hidden layers DNN, shown in Fig. 3, for hierarchical extraction of amplitude histograms' features which are subsequently exploited by DNN for MFI. The DNN is comprised of two autoencoders (acting as features

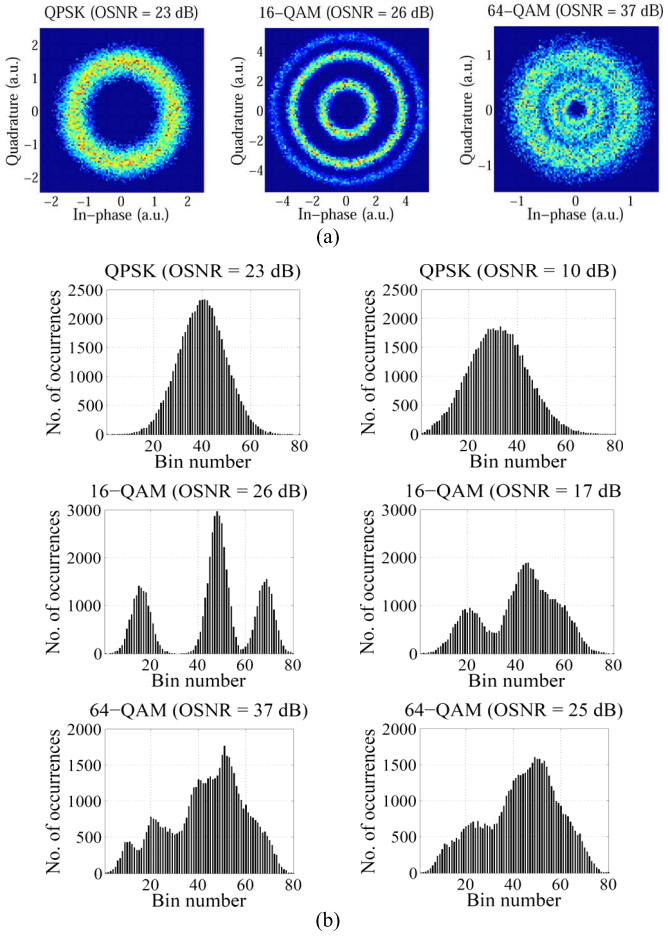


Fig. 2. (a) Constellation diagrams and (b) amplitude histograms at two different OSNRs, for the three modulation formats types under consideration.

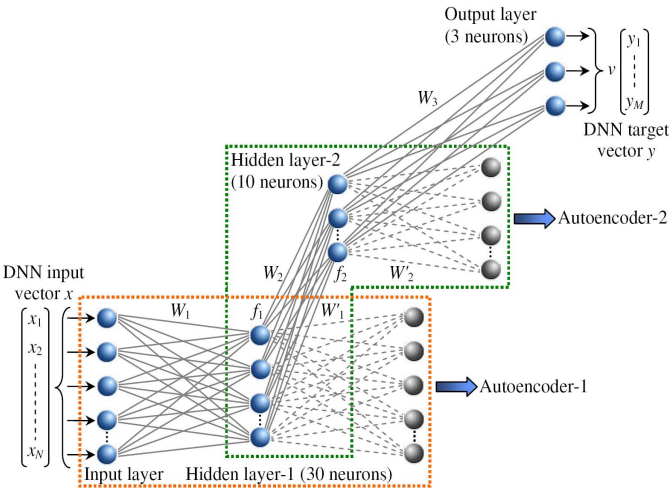


Fig. 3. Schematic diagram of a two hidden layers DNN. The second half of each autoencoder (called decoder) is depicted in grey color with dotted weight lines.

extractors) and an output perceptron layer. An autoencoder is essentially a feed-forward neural network which aims to learn the features of input data itself in order to obtain a compressed representation. The output layer of DNN is chosen to be a *softmax* layer due to its suitability for multiclass classification problems such as the one under consideration. For the training of DNN, a large data set comprising of numerous amplitude histograms, corresponding to three modulation formats and

various OSNRs, is obtained. Each histogram in the training data set is represented by an 80 × 1 vector $x$ of bin-counts. In addition, for each histogram, we generated a 3 × 1 binary vector $y$, called a label or target vector, with only one non-zero element whose location indicates actual modulation format of the signal. The vectors $x$ and $y$ pertaining to training data set are employed for the training of DNN. For this purpose, autoencoder-1 is first trained alone utilizing vectors $x$ in an unsupervised manner i.e. without using labels $y$. The autoencoder-1 attempts to replicate its input vectors $x$ at its output. Hence, the size of its output is equal to the size of its input as shown in Fig. 3. The first half of autoencoder-1 (called encoder) maps an input vector $x$ to a hidden representation while the second half (called decoder) attempts to reverse this mapping so as to reconstruct the original input $x$. If the number of neurons in hidden layer-1 is selected to be less than the size of input vectors $x$ (i.e. 80), the mapping learnt by encoder part of autoencoder-1 provides a compressed representation, called feature vectors $f_1$, of input vectors $x$. The decoder part of autoencoder-1 (shown in grey color) is then discarded and feature vectors $f_1$ are used for the unsupervised training of autoencoder-2 in isolation. The number of neurons in hidden layer-2 is chosen to be less than the size of vectors $f_1$ so that autoencoder-2 learns an even smaller representation of initial input vectors $x$. The decoder part of autoencoder-2 is then dropped and a second set of feature vectors $f_2$ is extracted by passing the previous set through the encoder of autoencoder-2. The extremely reduced size feature vectors $f_2$ are utilized for the training of final output layer in a supervised manner i.e. by using labels $y$ of the training data set as target outputs. Once the three individual components of DNN are trained in isolation, a complete network is formed by cascading the encoders of two autoencoders and the output layer. Finally, back-propagation (BP) algorithm is applied to train the whole multilayer network one last time in a supervised fashion by using vectors $x$ and $y$ of the training data set. This step is often referred to as fine-tuning.

Once the training process of DNN is complete, its performance is analyzed by employing a separate and independent set of data called testing data set. For this purpose, bin-count vectors $x$ belonging to the testing data set are applied at the input of trained DNN. The location of largest element in each corresponding output vector $v$ i.e., argmax$\{v\}$ then gives the estimated modulation format type. The identified modulation formats are compared with true ones i.e., the ones provided by labels $y$ of the testing data set and the estimation accuracies are computed.

## III. Experimental Setup and Results

The experimental setup used is shown in Fig. 4. A 150 kHz-linewidth external cavity laser (ECL) operating at 1550.12 nm is used to provide carrier signal to in-phase/quadrature (I/Q) modulators which are driven by multilevel electrical signals to generate 28 Gbaud QPSK, 14 Gbaud 16-QAM, and 20 Gbaud 64-QAM optical signals. Polarization multiplexing is then achieved by employing polarization beam splitters (PBSs), optical delay lines, and polarization beam combiners (PBCs) to obtain 112 Gbps PM QPSK, 112 Gbps PM 16-QAM, and

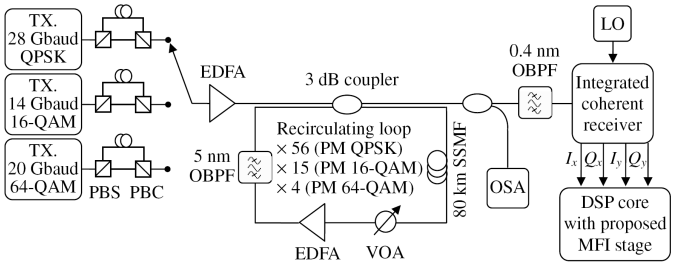


Fig. 4. Experimental setup used for DNN-based MFI in digital coherent receivers.

240 Gbps PM 64-QAM signals. The amplified optical signals are transmitted over a fiber recirculating loop comprising of an 80 km span of standard single-mode fiber (SSMF), an erbium-doped fiber amplifier (EDFA), a variable optical attenuator (VOA) for adjusting OSNR, and an optical band-pass filter (OBPF) for equalizing channel power. The OSNRs of PM QPSK, PM 16-QAM, and PM 64-QAM signals are altered in the ranges of 10−23 dB, 17−26 dB, and 25−37 dB, respectively, in steps of ∼1 dB. The OSNR ranges considered in this work are the ones used practically for reliable data transmission with the abovementioned signal types. At the loop output, the optical signals are first filtered by a 0.4 nm bandwidth OBPF to remove the redundant noise present in the signals and then coherently detected by an integrated coherent receiver. The linewidth of local oscillator (LO) laser is 100 kHz while the frequency offset between transmitter and LO lasers is around 1 GHz. The bandwidth of analog front-end of the receiver is 22 GHz. The coherently detected signals are sampled using a 50 Gsamples/s oscilloscope to collect 56,000 samples which are then processed offline utilizing the DSP core shown in Fig. 1. The polarization de-multiplexed signals obtained after CMA equalization stage are used to synthesize amplitude histograms with 80 bins as shown in Fig. 2(b). In this work, we acquired a large data set of 195 histograms corresponding to three modulation formats and various OSNRs. Two distinct subsets i.e. training and testing data sets are then generated by randomly choosing 68% (i.e. 135) and 32% (i.e. 60) histograms, respectively, from the original data set. For each histogram in the two data sets, vector pairs ($x$, $y$) are obtained which are then utilized for the training and testing of DNN using the procedure discussed in previous section.

Figure 5 depicts elements of DNN output vectors $v$ corresponding to 60 bin-count vectors $x$ in the testing data set. It is evident from the figure that for each test case, one specific element of $v$ has substantially larger value than the others. The clear separation between the largest element in $v$ and the rest indicates that there is no ambiguity faced by DNN in identifying the signals' modulation formats. Therefore, we can expect very high identification accuracies for the three signal types considered in this work. The MFI results for 60 test cases are summarized in Table I. It is obvious from the table that absolutely no errors are encountered in the identification of all three modulation formats thus resulting in an identification accuracy of 100%. We also analyzed the performance of MFI technique in the presence of fiber nonlinearity. For this purpose, the transmitted powers of PM QPSK and PM 16-QAM

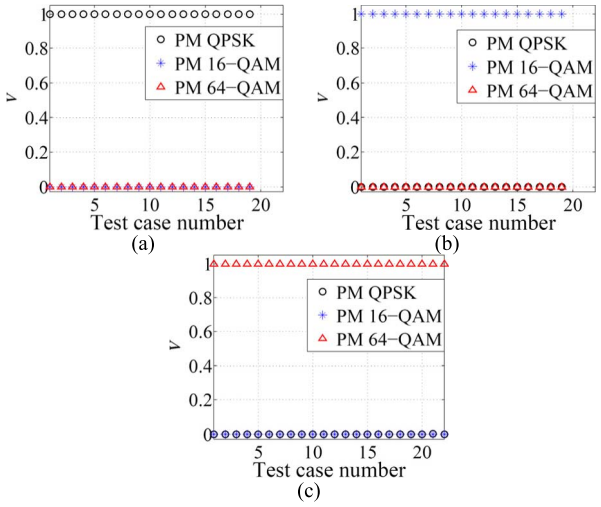


Fig. 5. Elements of DNN output vectors $v$ for (a) PM QPSK, (b) PM 16-QAM, and (c) PM 64-QAM modulation formats in response to 60 bin-count vectors $x$ in the testing data set.

TABLE I

CONFUSION MATRIX SHOWING THE PERFORMANCE OF PROPOSED TECHNIQUE FOR 60 TEST CASES IN THE TESTING DATA SET

| | | Identified Modulation Format | | |
|---|---|---|---|---|
| | | **PM QPSK** | **PM 16-QAM** | **PM 64-QAM** |
| **Actual Modulation Format** | **PM QPSK** | 19<br>100% | 0<br>0% | 0<br>0% |
| | **PM 16-QAM** | 0<br>0% | 19<br>100% | 0<br>0% |
| | **PM 64-QAM** | 0<br>0% | 0<br>0% | 22<br>100% |

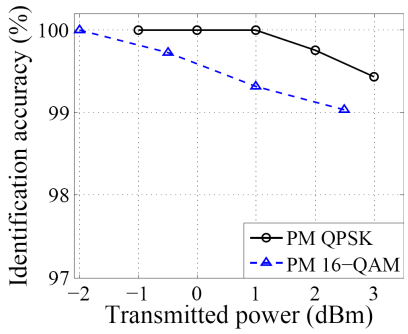


Fig. 6. Effect of fiber nonlinearity on the identification accuracy of proposed technique.

signals are varied in the ranges of -1−3 dBm and -2−2.5 dBm, respectively. The experimental results are shown in Fig. 6. It is clear from the figure that though the identification accuracies decrease slightly in the presence of fiber nonlinearity, they still remain reasonably good thus showing the resilience of proposed technique against fiber nonlinear effects.

From the experimental results, the proposed MFI technique offers following main benefits over existing methods [3]–[7]. (i) Unlike [3], this technique performs MFI at an earlier stage of DSP chain and thus avoids the need for multiple modulation format-transparent algorithms. (ii) The proposed technique enables accurate MFI irrespective of signal's OSNR. This is in contrast to [4], [5] which require prior information about OSNR of the received signal. (iii) Unlike the method presented in [6], which necessitates extra hardware components, the proposed technique demonstrates MFI functionality using standard digital coherent receiver, thus avoiding additional implementation costs. (iv) Since this technique is non-iterative in nature, MFI can be accomplished quite fast thus making this method attractive for use in EONs involving rapid variations of modulation formats. On the other hand, the technique proposed in [7] employs an iterative algorithm which inherently requires significant computation time.

Note that apart from the signal types under consideration, the proposed MFI technique can also be applied to several other advanced multilevel modulation formats provided that their amplitude histograms are distinguishable from each other. Hence, one limitation of the proposed technique is that it can not differentiate between various $M$-PSK ($M \geq 4$) signals since they produce similar amplitude histograms.

## IV. CONCLUSION

In this letter, we proposed the use of DNN in combination with signals' amplitude histograms for NDA MFI in digital coherent receivers. The experimental results demonstrated good identification accuracies for three commonly-used modulation formats despite having no prior OSNR information. The proposed technique follows a non-iterative approach and avoids any additional hardware components. Therefore, it is ideal for fast and cost-effective MFI in future EONs.

## REFERENCES

[1] O. Gerstel, M. Jinno, A. Lord, and S. J. B. Yoo, "Elastic optical networking: A new dawn for the optical layer?" *IEEE Commun. Mag.*, vol. 50, no. 2, pp. s12–s20, Feb. 2012.

[2] Z. Dong, F. N. Khan, Q. Sui, K. Zhong, C. Lu, and A. P. T. Lau, "Optical performance monitoring: A review of current and future technologies," *J. Lightw. Technol.*, vol. 34, no. 2, pp. 525–543, Jan. 15, 2016.

[3] N. G. Gonzalez, D. Zibar, and I. T. Monroy, "Cognitive digital receiver for burst mode phase modulated radio over fiber links," in *Proc. Eur. Conf. Opt. Commun. (ECOC)*, Torino, Italy, Sep. 2010, pp. 1–3.

[4] P. Isautier, K. Mehta, A. J. Stark, and S. E. Ralph, "Robust architecture for autonomous coherent optical receivers," *IEEE J. Opt. Commun. Netw.*, vol. 7, no. 9, pp. 864–874, Sep. 2015.

[5] J. Liu, Z. Dong, K. Zhong, A. P. T. Lau, C. Lu, and Y. Lu, "Modulation format identification based on received signal power distributions for digital coherent receivers," in *Proc. Opt. Fiber Commun. Conf. (OFC)*, San Francisco, CA, USA, Mar. 2014, pp. 1–3.

[6] S. M. Bilal, G. Bosco, Z. Dong, A. P. T. Lau, and C. Lu, "Blind modulation format identification for digital coherent receivers," *Opt. Exp.*, vol. 23, no. 20, pp. 26769–26778, Oct. 2015.

[7] R. Borkowski, D. Zibar, A. Caballero, V. Arlunno, and I. T. Monroy, "Stokes space-based optical modulation format recognition for digital coherent receivers," *IEEE Photon. Technol. Lett.*, vol. 25, no. 21, pp. 2129–2132, Nov. 1, 2013.

[8] Y. Bengio, "Learning deep architectures for AI," *Found. Trends Mach. Learn.*, vol. 2, no. 1, pp. 1–127, Nov. 2009.

[9] T. Serre, G. Kreiman, M. Kouh, C. Cadieu, U. Knoblich, and T. Poggio, "A quantitative theory of immediate visual recognition," *Prog. Brain Res.*, vol. 165, pp. 33–56, Oct. 2007.

[10] F. N. Khan, Y. Zhou, A. P. T. Lau, and C. Lu, "Modulation format identification in heterogeneous fiber-optic networks using artificial neural networks," *Opt. Exp.*, vol. 20, no. 11, pp. 12422–12431, May 2012.

[11] M. C. Tan, F. N. Khan, W. H. Al-Arashi, Y. Zhou, and A. P. T. Lau, "Simultaneous optical performance monitoring and modulation format/bit-rate identification using principal component analysis," *IEEE J. Opt. Commun. Netw.*, vol. 6, no. 5, pp. 441–448, May 2014.

[12] F. N. Khan *et al.*, "Experimental demonstration of joint OSNR monitoring and modulation format identification using asynchronous single channel sampling," *Opt. Exp.*, vol. 23, no. 23, pp. 30337–30346, Nov. 2015.